# Competing density-wave orders in a one-dimensional hard-boson model

Paul Fendley
*Department of Physics, University of Virginia, Charlottesville, VA 22904-4714*

K. Sengupta and Subir Sachdev
*Department of Physics, Yale University, P.O. Box 208120, New Haven CT 06520-8120*

(Dated: February 2, 2008)

We describe the zero-temperature phase diagram of a model of bosons, occupying sites of a linear chain, which obey a hard-exclusion constraint: any two nearest-neighbor sites may have at most one boson. A special case of our model was recently proposed as a description of a "tilted" Mott insulator of atoms trapped in an optical lattice. Our quantum Hamiltonian is shown to generate the transfer matrix of Baxter's hard-square model. Aided by exact solutions of a number of special cases, and by numerical studies, we obtain a phase diagram containing states with long-range density-wave order with period 2 and period 3, and also a floating incommensurate phase. Critical theories for the various quantum phase transitions are presented. As a byproduct, we show how to compute the Luttinger parameter in integrable theories with hard-exclusion constraints.

## I. INTRODUCTION

In recent years, the study of quantum models with multiple competing ground states has emerged as an important theme in the study of strongly-correlated many-body quantum systems. For example, in the cuprates it is clear that states with density-wave order at a variety of wavevectors play an important role in the physics at low carrier concentrations.

In this paper, we introduce a simple one-dimensional quantum model which displays a multiplicity of ground states. Despite its simplicity, it exhibits (*i*) gapped states with commensurate density-wave order (with periods of 2 and 3 lattice spacings), (*ii*) gapless regions with "floating" incommensurate, quasi-long-range density-wave correlations, and (*iii*) gapped states which preserve translational symmetry. A special case of our model appeared in a recent study [1] of atoms trapped in optical lattices [2], and so an experimental study of the phase diagram presented here may be feasible. More generally, we offer our model as a simple laboratory, with many exactly solvable cases, for the interplay of density-wave orders with multiple periods in quantum systems.

Our model is expressed in terms of the bose operator $d_j$, which annihilates a boson on site $j$, and the boson number operator

$$n_j \equiv d_j^\dagger d_j. \tag{1}$$

The "hard" boson condition allows no more than 1 boson on any pair of nearest-neighbor sites, and hence all states obey the constraints

$$n_j \leq 1 \quad ; \quad n_j n_{j+1} = 0. \tag{2}$$

In the study of Mott insulators in optical lattices [1], the $d_j$ boson represents a *dipole* excitation, consisting of a particle-hole pair bound on nearest neighbor sites of the optical lattice. This microscopic dipole interpretation will not be crucial to our analysis here, and so we will refer to $d_j$ simply as a boson.

The boson Hamiltonian we study is

$$\mathcal{H} = \sum_j \left[ -w \left( d_j + d_j^\dagger \right) + U n_j + V n_j n_{j+2} \right] \tag{3}$$

Note that the total number of bosons is not conserved, and it is possible to create and annihilate bosons out of the vacuum. This is natural in the dipole interpretation of the boson, as a particle-hole pair can be created or annihilated from the background Mott insulator. There is also no explicit boson hopping term; as was shown in Ref. 1, boson hopping is generated by the combination of the constraints in (2) and single-site terms already in $\mathcal{H}$, and so it is not necessary to include an explicit hopping. $U$ is a chemical potential for the bosons, while $V$ is a "nearest"-neighbor interaction, "nearest" meaning two sites apart, the closest two bosons can come. One can of course rescale out one of the couplings to obtain a two-parameter Hamiltonian, but it will be convenient to keep all three. The case $V = 0$ of $\mathcal{H}$ was studied in Ref. 1; we have also streamlined the earlier notation of the coupling constants to a form suitable for our analysis here. Without the constraints (2), the Hamiltonian would be trivially solvable. With them, its analysis becomes quite intricate.

The ground state of our Hamiltonian (3) can exhibit several kinds of order, depending on the couplings. The Hamiltonian will favor having bosons on every other site if we have an attractive "nearest"-neighbor interaction, or a chemical potential favoring the creation of particles. We will show that this leads to a regime of Ising-type order, with a spontaneously broken $\mathbf{Z_2}$ symmetry, translation by one site. If the chemical potential still favors creating particles, but there is a repulsive "nearest" neighbor potential, then the ground state will favor having a particle on every third site. This sort of order breaks a $\mathbf{Z_3}$ symmetry, translation by one or two sites.

When the the two kinds of ordered states have nearly the same energies, we will show that there exists an incommensurate phase. In the incommensurate phase, bosons appear on every other or every third site.

The one-dimensional quantum Hamiltonian (3) looks unusual because of the single-particle creation and annihilation operators. However, it in fact has already appeared in a very different context: it arises from taking the (Euclidean) time continuum limit of a two-dimensional classical statistical-mechanical model, the hard-square model [3]. This model describes the statistical mechanics of square tiles placed on the sites of a square lattice. Each square tile is rotated by 45° from the principal axes of the square lattice, and the area of each tile is twice the area of a single plaquette of the lattice. Tiles are not allowed to overlap, so this means nearest-neighbor sites cannot both be occupied: putting a tile on every other site of the square lattice covers all of space.

It is easy to see that the Hilbert space of our one-dimensional quantum theory is identical to the space of states along a line of the hard-square model. In the quantum theory, the Hilbert space consists of bosons which are restricted one to a site and forbidden to be nearest neighbors. In the two-dimensional classical theory, the squares appear at most one to a site, and are forbidden to be nearest neighbors. It is less obvious that one can obtain the quantum Hamiltonian (3) by taking a limit of the classical transfer matrix. We show in the Appendix how to do this, by taking the (Euclidean) time direction to be along the diagonals of the square lattice. Roughly speaking, the chemical potential $U$ and interaction $V$ correspond to a chemical potential and interaction strength for the squares. The precise relations are derived in the Appendix.

The phase diagram of the hard-square model has been studied in Ref. 4. We will explain in section II how these results apply to the ground state of our quantum Hamiltonian. An extremely useful result is that the hard-square model is integrable for some values of the Boltzmann weights [3]. In terms of the Hamiltonian (3), this amounts to two lines in our two-parameter space of couplings:

$$w^2 = UV + V^2. \tag{4}$$

There is a single critical point along each of these lines; they are in the universality classes of the Ising tricritical point and of the three-state Potts model critical point. We will show how these critical points describe transitions to and from the $\mathbf{Z}_2$ and $\mathbf{Z}_3$ ordered phases.

In section II we discuss the different regions of phase space. In section III we discuss in depth the phase with order of period 3, the phase with spontaneously-broken $\mathbf{Z}_3$ symmetry. We present numerical results to support the analytic arguments. In sections IV and V, we discuss the incommensurate "floating" phase in depth. In section IV we derive an effective Hamiltonian for this region, and prove that an incommensurate phase exists by bosonizing it. In section V we calculate the size of this phase by using the Bethe ansatz to compute the effective Luttinger parameter exactly. This enables us to find the region in which vortex-type perturbations are irrelevant and do not destroy the incommensurability. Unfortunately, this region occupies a fairly small region of parameter space, so it is not possible to see this result numerically.

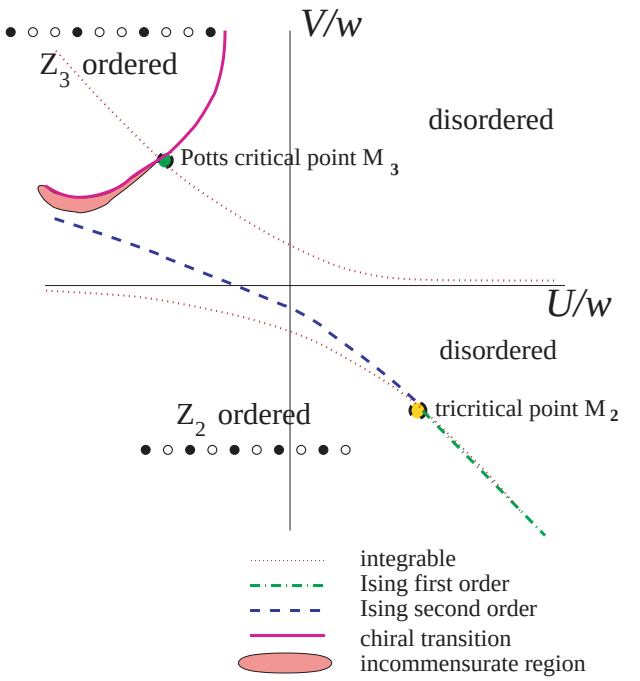


FIG. 1: Ground-state phase diagram of $\mathcal{H}$ as a function of $U/w$ and $V/w$. Schematic representations of the ground states with density waves of period 2 and 3 are shown. The dotted lines indicate the positions of the integrable lines in (4). The critical points along these lines (6,8) are labeled $M_{2,3}$. The extent of the incommensurate region has been greatly exaggerated for clarity: it is drawn to scale in Fig 8. There could also be an incommensurate region adjacent to the chiral transition line about $M_3$, but we have no direct evidence for this possibility.

## II. PHASE DIAGRAM

Our main results are summarized in the phase diagram shown in Fig 1. We discuss the phases and phase transitions in this figure by considering a number of limiting cases.

### A. $\mathbf{Z}_2$ order

First we consider the case $V = 0$, which was studied earlier in Ref. 1. Although the Hamiltonian looks simple in this limit, the prohibition of nearest-neighbor bosons means that this case is not solvable except as

$U/w \to \pm\infty$. For large positive $U/w$ we obtain a featureless ground state with a small density of bosons and which breaks no translational symmetry, as is easily seen from $\mathcal{H}$. This is a disordered, or liquid, phase. Similarly, for $U/w$ large and negative, the energy is minimized by states with a maximal density of bosons: there are 2 degenerate states of this type, each with every second site occupied; in other words, there is a density wave of period 2, and translational symmetry is spontaneously broken. It was shown numerically in Ref. 1 that there is a second-order Ising critical point which separates these phases at $U/w = -1.308\ldots$.

One can also find the location of the transition from Ising order to disorder easily in the limit $V \to -\infty$ and $U \approx -V$. With $|U|$ and $|V|$ both large, we can ignore the $w$ term, and then $\mathcal{H}$ becomes a model of classical particles. The empty state with no particles has energy 0, while the maximally occupied states with density waves of period 2 have energy per lattice site of $(U+V)/2$. There is therefore a first-order transition between these states at $U = -V$. Actually, it is quite easy to find the position of this first-order transition to order $(w/V)^2$. Using standard second-order perturbation theory in $w$, the energy per site of the empty state is $-w^2/U$. Similarly, the energy per site of the maximally occupied state is $(U+V)/2 + w^2/(2(U+2V))$. Equating these two energies we estimate the position of the first-order transition to be

$$\frac{U}{V} = -1 + \frac{w^2}{V^2} \tag{5}$$

The integrability of the model along the lines (4) lets us understand how this transition occurs at finite $V$ and $w$. In fact, the condition (5) coincides precisely with one of the integrable lines in (4). Indeed, the arguments of Huse [4] and the exact results [3, 5] imply that integrable line is precisely along the co-existence line of these two phases, and hence the first-order boundary is given exactly by (5), with no corrections at higher order in $w/V$.

At the value

$$\frac{V}{w} = -\left(\frac{\sqrt{5}+1}{2}\right)^{5/2} \tag{6}$$

there is a critical point along the integrable line. Thus the first-order transition line must terminate. Huse argued that this integrable quantum critical point was a tricritical point separating a first-order boundary from a line of second-order Ising transitions. Indeed, the computation of exact critical exponents at this point [3, 5] shows that this critical point in the hard-square model is in the same universality class as the tricritical point in the Ising model. This tricritical point in the continuum limit is described by the minimal conformal field theory with central charge $c = 7/10$ [6]. Therefore, the line of first-order transitions determined by (5) is present for $V/w < -((\sqrt{5}+1)/2)^{5/2}$, where it terminates at the Ising tricritical point $M_2$ shown in Fig 1. There is a line of second-order Ising transitions on the other side of $M_2$, but this is *not* on the integrable line (4); this second-order line clearly passes through the point (6) discussed above. The exact computations show that the integrable line for $0 > V/w > -((\sqrt{5}+1)/2)^{5/2}$ is in the $\mathbf{Z}_2$ ordered phase [3, 5]. This is consistent with the finite value (6) of $U_c$ for $V = 0$; at $V = 0$ the integrable line is at $U = -\infty$.

### B. $\mathbf{Z}_3$ order

Consider the case $V \to \infty$, $|U| \ll V$. The large positive value of $V$ now prohibits bosons separated by 2 lattice spacings, and hence we effectively have the constraint

$$n_j n_{j+2} = 0 \tag{7}$$

along with the constraints (2). The physics in this region can be understood using reasoning parallel to that in Section II A. As before, for large positive $U/w$, we obtain a featureless ground state with a small density of bosons, which breaks no lattice symmetry. For $U/w$ large and negative, the ground state has a maximal density of bosons: with the constraints (2) *and* (7) there are now 3 degenerate states of this type, each with every third site occupied. Here we thus have a density wave of period 3.

To study this phase with spontaneously-broken $\mathbf{Z}_3$ symmetry at finite $V$, we can use results for the other integrable line, where $V/w > 0$ in (5). Along this line there is a quantum critical point at [3]

$$\frac{V}{w} = \left(\frac{\sqrt{5}+1}{2}\right)^{5/2}. \tag{8}$$

This critical point is in the universality class of the three-state Potts model [3, 5]. In the continuum limit this is described by the minimal conformal field theory with central charge 4/5 [6]. For $w/V$ smaller than this value and along this line, the exact results indeed show that the $\mathbf{Z}_3$ translation symmetry is broken. For $w/V$ larger than this value and along this line, there is no order. Thus along the integrable line, the transition is in the universality class of the usual order-disorder transition in the three-state Potts model; similar $\mathbf{Z}_3$ quantum criticality occurs in an XXZ chain in a staggered field [7]. However, as opposed to the Ising case, the transition away from this integrable line is not of the usual type [4]: it is related that of the chiral clock model [8]. We will discuss the nature of the transition between these states as a function of $U/w$ in Section III, including the possibility of additional intermediate states with incommensurate periods.

### C. Competing orders

The most complicated and interesting limit is $V \to \infty$, $U \approx -3V$. where there is competition between density-wave orders of period 2 and period 3. Initially, as in

Section II A, we anticipate that with $|V/w|$ and $|U/w|$ both large, we can neglect quantum effects and consider a model of classical particles. The period-2 and period-3 density-wave states then have energies per site $(U+V)/2$ and $U/3$ respectively, so that the ground states become degenerate at $U = -3V$. In fact, at $U = -3V$ in this limit, there are many degenerate states: any state where successive particles are separated by either 2 or 3 lattice spacings is within the ground state manifold. This results in an extensive classical entropy at $U = -3V$. This extensive degeneracy is lifted only by quantum effects, and perturbation theory in $w$ is therefore highly non-trivial. The analysis of quantum effects in this regime will be presented in Sections IV and V. We will establish that there is an intermediate gapless phase with incommensurate spin correlations. We will show as well that the gapped state with no broken symmetry also intervenes between the period-2 density-wave state and the incommensurate phase, as shown in Fig. 1.

We will argue in Section III that there also should be an incommensurate phase near the Potts critical point $M_3$. The simplest and most plausible possibility is that this phase and the one for $-U \approx 3V \gg 1$ are the same. We have drawn the phase diagram in this fashion.

## III. DENSITY-WAVE ORDER OF PERIOD 3

The density-wave state of period 3 appears when $V$ is large and positive, so that bosons with separations of both 1 and 2 lattice spacings are suppressed. This section and the next will discuss the manner in which quantum fluctuations destroy this period-3 order.

It is useful to begin with the limit $V \to \infty$, noted above in Section II B. At first glance, there appear to be only two distinct possibilities for the ground states: a featureless, low density state at large positive $U/w$, and a density-wave state of period 3 at large negative $-U/w$. We might also anticipate that these states are separated by a second-order critical point in the universality class of the 3-state Potts model. However, the situation is more subtle [4].

It is useful to introduce order parameters, $\Psi_p$, which characterize density-wave orders of period $p$ (in general, $p$ need not be an integer):

$$\Psi_p = \sum_j n_j e^{i2\pi j/p} \tag{9}$$

For $p = 2$, the Ising order parameter $\Psi_2$ is real. However, for the $p = 3$ case we consider in this section, the Potts order parameter $\Psi_3$ is complex. Clearly, the state with density wave order of period 3 has $\langle \Psi_3 \rangle \neq 0$, while the featureless, low density state has $\langle \Psi_3 \rangle = 0$.

Using the usual symmetry criteria, we can write down a continuum quantum field theory describe the onset of Potts order. The action should be invariant under translations, under which $\Psi_3 \to e^{i2\pi\ell/3}\Psi_3$, with $\ell$ integer. A crucial point, noted by Huse and Fisher [9] in a different context, is the behavior under spatial inversion:

$$x \to -x \quad , \quad \Psi_3 \to \Psi_3^* \tag{10}$$

where $x$ is the continuum spatial co-ordinate. Finally, we note that $\Psi_3$ is invariant under time reversal. These symmetry constraints lead to the following proposed effective action for the quantum field theory ($\tau$ is imaginary time):

$$\begin{aligned} \mathcal{S}_3 \;=\; & \int dx d\tau \left[ i\alpha \Psi_3^* \partial_x \Psi_3 + \text{c.c} + |\partial_\tau \Psi_3|^2 + v^2 |\partial_x \Psi_3|^2 \right. \\ & \left. +\; r|\Psi_3|^2 + v\Psi_3^3 + \text{c.c.} + \ldots \right] \end{aligned} \tag{11}$$

The critical point associated with this field theory occurs at $\alpha = r = 0$, and is in the same universality class as the critical point in the three-state Potts model. This is described by a conformal field theory of central charge 4/5, and the dimensions of all the operators are known.

The exact results show that the integrable critical point $M_3$ indeed is in the universality class of the three-state Potts model [3, 5]. It separates a state with density-wave order of period 3 from the gapped translationally-invariant state [3, 6]. Just because the critical point is in the same universality class as the three-state Potts model does not mean that all the physics in the region of the critical point is the same. The key difference is the presence here of the linear spatial derivative proportional to $\alpha$, which is clearly allowed under the symmetries (10). This term is *chiral*, in that it breaks rotational symmetry. The exact results show no evidence of chiral behavior, so the effective theory describing the integrable line presumably corresponds to $\alpha = 0$. Varying $r$ at $\alpha = 0$ therefore moves one along the integrable line, and describes the usual physics of the three-state Potts model: a second-order transition between $\mathbf{Z}_3$ order and disorder.

When one moves off the integrable line (taking $\alpha \neq 0$ in the effective theory), the theory in the universality class of the *chiral clock model* [8]. The chiral perturbation, $\alpha$, is known to be relevant at the ordinary Potts critical point [10], with scaling dimension 1/5; the perturbing operator has dimensions 9/5 and breaks Lorentz invariance. Thus for $\alpha \neq 0$, the quantum phase transition associated with the vanishing of density-wave order of period 3 is in general *not* in the same universality class as the usual order/disorder transition in the ordinary 3-state Potts model. The integrable point $M_3$ is an isolated multicritical point; all other points on the phase boundary of the period-3 state must have $\alpha \neq 0$, and display the physics of the chiral clock model. Note the contrast with the corresponding transition associated with density-wave order of period 2: this transition is in the Ising universality class because $\Psi_2$ is real, and then the term proportional to $\alpha$ is a vanishing total derivative.

The chiral clock model is generally believed to exhibit an incommensurate phase [8, 9, 10]. In the region near the multicritical point $M_3$, this occurs when the chiral perturbation ($\alpha \neq 0$) dominates over the thermal perturbation ($r \neq 0$). This region is therefore quite narrow,

because $\alpha$, of dimension 1/5, is much less relevant than $r$, which is of dimension 6/5. Thus $r$ must effectively vanish for the effects of the chiral perturbation to be felt. In the next section, we will show that the incommensurate phase does have a finite (albeit small) width far from the multicritical point, where $|U|$ and $V$ are large, with $U = \approx V/3$. There is no indication that any more new physics intervenes in between this region and the incommensurate region near $M_3$, so we presume that these two phases are the same, as we have indicated in Fig. 1.

In the remainder of this section we will describe our numerical study of the physics in the limit $V \to \infty$, which corresponds to being on the portion of the phase boundary of the period-3 state *above* the multicritical point $M_3$ in Fig 1. Our numerical results here are inconclusive, as we see little deviation from the pure 3-state Potts physics for the system sizes examined. We will study the portion of the phase boundary *below* $M_3$ in Section IV, and there we shall definitively establish the existence of a gapless incommensurate phase, driven by the presence of the chiral perturbation; the ordering wavevector, $K = 2\pi/p$, of this incommensurate phase obeys $K > 2\pi/3$. A simple fluctuation analysis of $\mathcal{S}_3$ indicates that $K - 2\pi/3$ is proportional to $\alpha$. As $\alpha$ vanishes at $M_3$ where $K = 2\pi/3$, these results suggest the conjecture that there is a small intermediate, gapless, incommensurate phase also above the point $M_3$, but with a change in sign of $\alpha$ leading to an ordering wavevector $K < 2\pi/3$. Our numerical studies below, however, do not show any specific evidence in support of this conjecture. This is possibly because the scaling dimension of the chiral perturbation is quite small, and very large system sizes are needed before its effects are perceptible. Furthermore, we shall find in the study of the portion of the phase boundary below $M_3$ in Section IV that the region of incommensurate spin correlations is extremely small, and it is likely that a similar feature holds in the above $M_3$ region being studied here.

The numerical analysis for large $V$ is simplified by simply eliminating all states with an energy determined by $V$. This is equivalent to extending the constraints (2) to

$$n_j \leq 1 \quad ; \quad n_j n_{j+1} = 0 \quad ; \quad n_j n_{n+2} = 0, \tag{12}$$

and working with the simplified Hamiltonian

$$\mathcal{H}_s = \sum_j \left[ -w \left( d_j + d_j^\dagger \right) + U n_j \right] \tag{13}$$

The exact diagonalization of $\mathcal{H}_p$ can then be carried out for system sizes $N \leq 21$.

First, we searched for the preferred values of $p$ in a system of size $N = 21$. We applied a small external cosine potential on the bosons of magnitude $10^{-4}$ and wavevector $2\pi/p$, and measured the resulting values of $\langle \Psi_p \rangle$ as a function of $U/w$. The results are shown in Figs 2 and 3. Fig. 2 shows that value of $\Psi_3$ is much larger than the response at another nearby wavevector. Figure 3 shows similar data, but with a greatly expanded vertical scale. The response at periods $p \neq 3$ is always

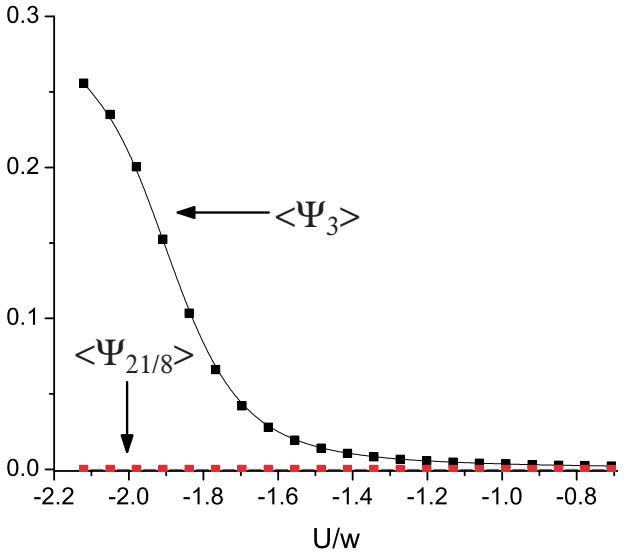


FIG. 2: Density-wave order, $\langle \Psi_p \rangle$, induced by an external potential at wavevector $2\pi/p$ and magnitude $10^{-4}$. There appears to be onset of spontaneous density-wave order with period $p$ at the smaller values of $U/w$.

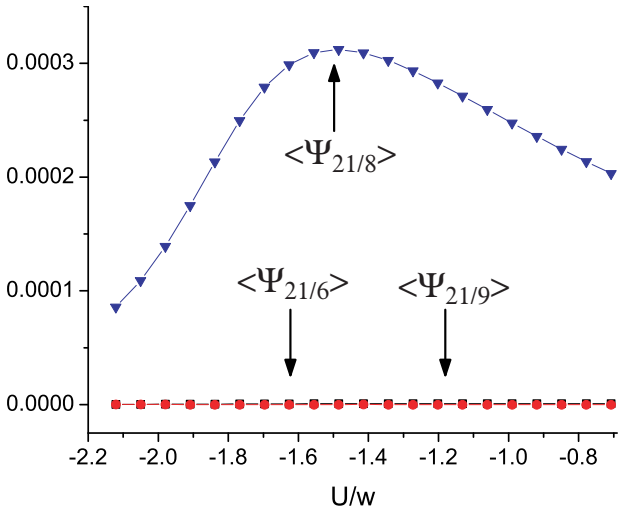


FIG. 3: As in Fig. 2, but with a greatly expanded vertical scale. All of the periods shown above show no sign of spontaneous order.

*much* smaller, and so we see no sign of spontaneous order at any other wavevectors. Interestingly, the largest secondary response is at the wavevector $16\pi/21$. This is contrary to our expectations earlier based on the influence of the chiral perturbation in (11), where we anticipated incommensurate order at wavevectors smaller than $2\pi/3$. However, given the very small susceptibility, and the small system sizes considered we are not able to interpret any of this data in support of an incommensurate phase. Any such phase, if present, must be over an extremely small parameter regime, as is found in Section IV

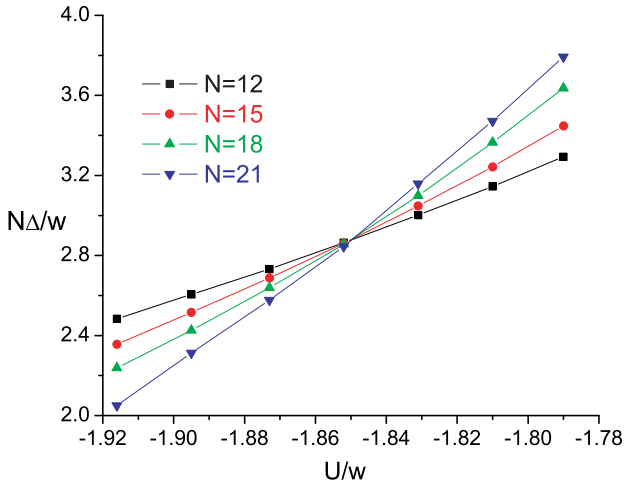


FIG. 4: Plot for the energy gap $\Delta$ as a function of $U$ for different system sizes. The data for different system sizes cross at $U_c/w = -1.852$.

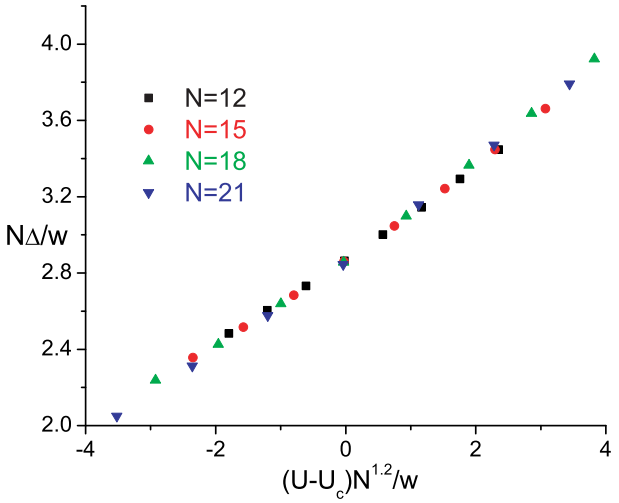


FIG. 5: Scaling plot for the energy gap $\Delta$. The data for different system sizes collapse for $\nu = 0.83$ and $U_c/w = -1.852$.

Ignoring the presence of a possible intermediate incommensurate phase, we now see if our data can be interpreted in the context of a direct transition from the gapped density-wave state of period 3, to a gapped "liquid" state which does not break any translational symmetries. We expect such a transition to be in the Potts universality class. Indeed, we now show that our data are in complete accord with such an assumption, with excellent agreement to the expected values of the critical exponents. This is again consistent with an as yet undetected influence of the chiral perturbation in the present analysis (the chiral perturbation is more clearly detected in Section IV).

First, let us determine the position of a presumed critical point from the period-3 (Potts) density-wave state to a disordered state using finite size scaling analysis. Near the quantum critical point, the energy gap $\Delta$ is expected to obey the scaling relation

$$\Delta \;=\; N^{-z}\Phi\left(N^{1/\nu}(U-U_c)\right) \qquad (14)$$

where $\Phi$ is an universal scaling function, $z$ is the dynamic critical exponent, and $\nu$ is the correlation length exponent. Fig. 4 shows a plot of $N\Delta/w$ vs $U/w$ which exhibits a clear crossing point at

$$\frac{U_c}{w} = -1.852. \qquad (15)$$

From Eq. 14, we thus conclude that $z = 1$. Fig 5 shows a plot of $N\Delta/w$ vs $N^{1.2}(U-U_c)/w$. We find that the data for all $N$ collapses for $U_c/w = -1.852$, giving $\nu = 0.833$. The numerical values of $\nu$ and $z$ obtained here are in excellent agreement with the known analytical values $z = 1$ and $\nu = 5/6$ for the three-state Potts model [17].

As a final test of the three-state Potts universality class, we calculate the equal-time structure factor of the

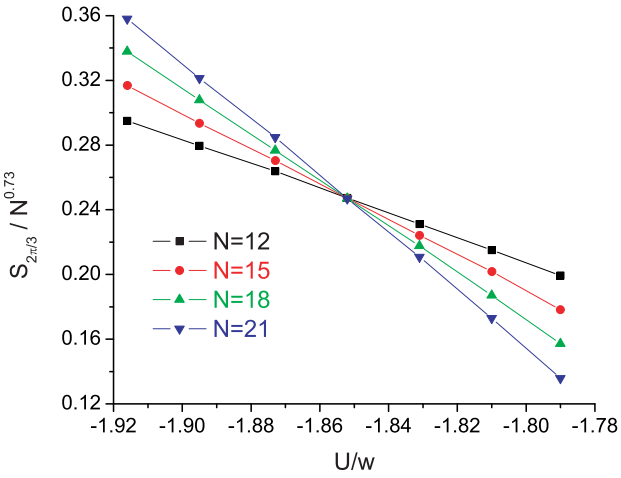


FIG. 6: Plot of the equal-time structure factor $S_{2\pi/3}$ for different system sizes. The data for different system sizes cross at $U_c/w = -1.852$ for $\eta = 0.27$

Potts order parameter $\Psi_3$ (Eq. 9) given by

$$S_{2\pi/3} \;=\; \frac{1}{N}\left\langle \Psi_3^* \Psi_3 \right\rangle . \qquad (16)$$

The structure factor is expected to scale as $N^{2-z-\eta}$ near the critical point. A plot of $S_{2\pi/3}/N^{0.73}$ vs $U/w$, as shown in Fig. 6, shows excellent crossing at $U_c/w = -1.852$. From this, knowing $z = 1$, we identify $\eta = 0.27$, which is again in good agreement with the known exact value $\eta = 4/15$ [17].

## IV. COMPETITION BETWEEN DENSITY-WAVE ORDERS OF PERIODS 2 AND 3: THE INCOMMENSURATE STATE

We noted in Section II C that in the classical limit ($w = 0$), the period-2 and period-3 states become degenerate for $U = -3V$. Here we shall study the quantum physics near this degeneracy point. As will become clear, the physics is quite complicated, but we are able to obtain a complete picture by a combination of perturbation theory, bosonization, and Bethe ansatz methods. Our primary result is that the gapped period-2 and period 3 are separated by 2 intermediate phases, and all these phases are separated by 3 second-order quantum phase transitions (see Fig. 1). Above the period-2 phase is the gapped, translationally invariant state, accessed by a conventional Ising transition. Above this is a gapless, incommensurate phase reached across a Kosterlitz-Thouless transition. Finally, we reach the gapped period-3 phase via a Pokrovsky-Talapov transition [11].

We will establish these results by a careful study of the region of the phase diagram where

$$0 < w, |U + 3V| \ll |U|, V \tag{17}$$

It will become clear from our analysis that the non-trivial region of the phase diagram is where

$$|U + 3V| \sim \frac{w^2}{V}. \tag{18}$$

So we introduce the new dimensionless coupling $\sigma$, and parameterize

$$U \equiv -3V \left[1 + \left(\frac{w}{V}\right)^2 \sigma\right]. \tag{19}$$

The above conditions on the interesting regime can now be restated as follows

$$0 < w \ll V \quad ; \quad \sigma \sim 1 \tag{20}$$

We shall follow the physics as $\sigma$ is tuned from large negative to large positive values, while maintaining (17).

### A. The effective Hamiltonian

As we mentioned in Section II C, under the condition (20), the important states are those in which successive $d_j$ bosons are separated by either 2 or 3 lattice spacings. We denote such a state by the sequence of lattice spacings *e.g.* $|\ldots 23323233\ldots\rangle$; see Fig. 7. We wish to develop an operator formalism for describing such states. We shall introduce two distinct formalisms below, but it should always be kept in mind that both describe identical Hilbert spaces with identical spectra.

In the first approach, we describe the states in terms of 'defects' or 'domain walls', or 'kinks' in the ordered period-2 density-wave states. This description focuses on the 3's in a background of 2's. We view each 3 as a new boson, created by the operator $t_\ell^\dagger$, located at the center of the 3 defect. Note that the $\ell$ sites lie at the midpoints of the links of the $j$ sites of the original model $\mathcal{H}$. Thus the state $|\ldots 2223222\ldots\rangle$ represents a single $t$ boson. An arbitrary state in the low-energy subspace can be described by a configuration of $t$ bosons. The resulting $t$ boson states obey some constraints: there can only be at most one $t$ boson per site, and successive $t$ bosons must be separated by $3, 5, 7, 9, 11\ldots$ sites.

FIG. 7: The state $|\ldots 23322\ldots\rangle$. Filled circles are $d_j$ bosons, and empty circles have no bosons.

Second-order perturbation theory also allows us to obtain the effective Hamiltonian for the $t$ bosons to order $(w/V)^2$. It is useful to first tabulate the energies of different configurations of the original $d$ bosons in different environments, to order $(w/V)^2$. For a $d$ boson between 22 bonds we have

$$E_{22} = U + V + \frac{w^2}{U + 2V}.$$

Similarly for a $d$ boson between 33 bonds we have

$$E_{33} = U + \frac{w^2}{U}.$$

Finally for a $d$ boson between 23 bonds we have

$$E_{23} = U + \frac{V}{2} + \frac{w^2}{U + V}.$$

From these expressions, we can obtain the energy of a $t$ boson well-separated from all other $t$ bosons:

$$\begin{aligned} E_t &= 2E_{23} - \frac{5}{2}E_{22} \\ &= V\left[\frac{3(1+\sigma)}{2}\left(\frac{w}{V}\right)^2 + \mathcal{O}\left(\frac{w}{V}\right)^3\right] \end{aligned}$$

Similarly, we obtain the interaction energy of two adjacent $t$ bosons

$$\begin{aligned} E_{t,\text{int}} &= 2E_{23} + E_{33} - 4E_{22} - 2E_t \\ &= V\left[-\frac{1}{3}\left(\frac{w}{V}\right)^2 + \mathcal{O}\left(\frac{w}{V}\right)^3\right] \end{aligned}$$

Finally, moving on to the $t$ boson hopping amplitude, a similar perturbation theory shows that it is $w^2/(U+V)$. Collecting all these results, we can now write down the effective Hamiltonian for the $t$ bosons, valid in the regime (20). On a system of $N$ sites the Hamiltonian $\mathcal{H}$ in (3) is effectively

$$\begin{aligned} \frac{\mathcal{H}_t}{V} &= -\frac{N}{2}\left(2 + (1+3\sigma)\left(\frac{w}{V}\right)^2\right) \\ &+ \left(\frac{w}{V}\right)^2 \sum_\ell \left[-\frac{1}{2}\left(t_{\ell+2}^\dagger t_\ell + t_\ell^\dagger t_{\ell+2}\right)\right. \\ &+ \left.\frac{3}{2}(1+\sigma)t_\ell^\dagger t_\ell - \frac{1}{3}t_{\ell+3}^\dagger t_{\ell+3} t_\ell^\dagger t_\ell\right] + \mathcal{O}\left(\frac{w}{V}\right)^3 \end{aligned} \tag{21}$$

We reiterate that $\mathcal{H}_t$ must be solved under the constraints that there can only be at most one $t$ boson per site, and successive $t$ bosons must be separated by $3, 5, 7, 9, 11 \ldots$ sites. To this order in $w/V$ the Hamiltonian conserves the number of $t$ bosons. Except for the latter constraint, this Hamiltonian is very much like that of an XXZ magnet. The hopping term in (22) is akin to spin exchange, the chemical potential is like an effective magnetic field $h_{eff} = 3(1+\sigma)/2$, and the interaction is akin to the $S_z S_z$ interaction between neighboring sites. The analogous (ferromagnetic) XXZ model has anisotropy $J_z/J_x = 1/3$, so it is in a gapless regime. We shall show in sect. V that this model is as well, for appropriate values of the effective magnetic field.

Before turning to analysis of $\mathcal{H}_t$, it is useful to introduce a complementary analysis of the physics valid under the conditions (20). Now, we consider defects or kinks between ordered states with period 3. So we treat the 2's as bosons moving in background 3's. Such bosons are created by the operator $p_j$, and note that this boson resides on the sites of the original lattice. The energy of an isolated $p$ boson is

$$\begin{aligned} E_p &= 2E_{23} - \frac{5}{3}E_{33} \\ &= V\left[-\left(\sigma + \frac{4}{9}\right)\left(\frac{w}{V}\right)^2 + \mathcal{O}\left(\frac{w}{V}\right)^3\right] \end{aligned}$$

Also, the interaction energy of two adjacent $p$ bosons is

$$\begin{aligned} E_{p,\mathrm{int}} &= 4E_{23} + E_{22} - 4E_{33} - 3E_p \\ &= V\left[-\frac{1}{3}\left(\frac{w}{V}\right)^2 + \mathcal{O}\left(\frac{w}{V}\right)^3\right] \end{aligned}$$

Finally, the hopping matrix element of the $p$ bosons is the same as that of the $t$ bosons. Collecting these results yields the following effective description of $\mathcal{H}$ in the regime (20):

$$\begin{aligned} \frac{\mathcal{H}_p}{V} &= -\frac{N}{3}\left(3 + \frac{(1+9\sigma)}{3}\left(\frac{w}{V}\right)^2\right) \\ &+ \left(\frac{w}{V}\right)^2 \sum_j \left[-\frac{1}{2}\left(p^\dagger_{j+3}p_j + p^\dagger_j p_{j+3}\right)\right. \\ &- \left.\left(\sigma + \frac{4}{9}\right)p^\dagger_j p_j - \frac{1}{3}p^\dagger_{j+2}p_{j+2}p^\dagger_j p_j\right] + \mathcal{O}\left(\frac{w}{V}\right)^3. \end{aligned} \tag{22}$$

The constraints on the $p$ bosons are that each site can have at most one $p$ boson, and successive $p$ bosons can only be separated by intervals of $2, 5, 8, 11, 14, \ldots$. Note that except for the constraints, this description also resembles a (ferromagnetic) XXZ model with the same anisotropy $\Delta = J_z/J_x = 1/3$.

It is important to note that the Hilbert space and spectra of $\mathcal{H}_t$ in (22) and $\mathcal{H}_p$ in (23) should be identical, although this is by no means obvious. Some simple consistency checks can however easily be performed: the vacuum state of $\mathcal{H}_t$ with no $t$ bosons should have the same energy as the state of $\mathcal{H}_p$ with the maximal number of $p$ bosons. The reader can easily check that this requirement, and its converse, do indeed hold. More generally, we can easily see from the manner in which we defined the states that if a state has $N_t$ $t$ bosons under $\mathcal{H}_t$, then the same state has $N_p$ $p$ bosons under $\mathcal{H}_p$ where

$$2N_p + 3N_t = N, \tag{23}$$

and $N$ is assumed to be a multiple of 6.

Some simple considerations now allow us to deduce some important properties of $\mathcal{H}_t$ and $\mathcal{H}_p$. Consider first the case $\sigma \gg 1$. A glance at $\mathcal{H}_t$ shows that each $t$ boson costs a large positive energy, and so the ground state is the $t$ boson vacuum (which also happens to be the state with the maximal number of $p$ bosons). This vacuum state is clearly the state with density state of period 2. The lowest excited state consists of a $t$ boson excitation (a kink), at zero momentum, which has an energy $(w^2/V)(1+3\sigma)/2$ above the ground state. So we conclude that the ground state remains a density wave of period 2 provided

$$\sigma > -\frac{1}{3} \quad \rightarrow \text{period-2 density-wave order} \tag{24}$$

This conclusion is illustrated in Fig. 8, which displays the final phase diagram emerging from the analysis of this section.

A similar argument can be applied to determine the stability of the period-3 density-wave state. From $\mathcal{H}_p$, this is stable for $\sigma \ll -1$. The energy of a single $p$ boson excited state at zero momentum is $-(w^2/V)(13+9\sigma)/2$, and so the ground state remains a density wave of period 2 provided

$$\sigma < -\frac{13}{9} \quad \rightarrow \text{period-3 density-wave order} \tag{25}$$

This is also shown in Fig. 8.

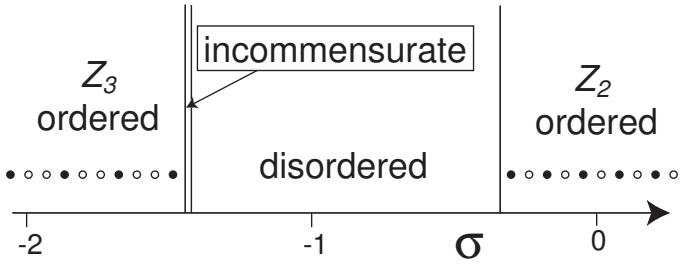


FIG. 8: Ground states of $\mathcal{H}$, $\mathcal{H}_t$, or $\mathcal{H}_p$ as a function of $\sigma$, under the conditions (20). The dimensionless coupling $\sigma$ is defined in (19); so the horizontal axis above corresponds to moving downward along the extreme left of Fig 1. The transition from the $Z_2$ ordered state to the disordered state at $\sigma = -1/3$ is in the Ising universality class, and has dynamic exponent $z = 1$. The $Z_3$ ordered state first undergoes a $z = 2$ transition to an incommensurate phase in the Pokrovsky-Talapov universality class at $\sigma = -13/9$, which is then followed by a $z = 1$ Kosterlitz-Thouless transition at $\sigma = -1.422...$ (this last number is determined from the Bethe ansatz analysis in Section V).

### B. Stability of the incommensurate phase

It now remains to understand the physics for $-13/9 < \sigma < -1/3$. The above considerations suggest that this intermediate region has a finite density of both $t$ and $p$ bosons obeying (23). If this is a compressible phase, then we expect the ground state to be a Luttinger liquid, and the corresponding correlations of the density of the underlying $d$ bosons to be incommensurate. Furthermore, the transition $\sigma = -13/9$ involving the onset of a nonzero density of the $p$ bosons would be a transition of the Pokrovsky-Talapov type [11], with dynamic critical exponent $z = 2$ [12], and an effective free fermion description near the critical point. Similar considerations can be expected to apply to the transition at $\sigma = -1/3$, associated with the onset of a finite density of $t$ bosons.

However, the validity of such a conclusion requires the absence of additional perturbations, at higher order in $w/V$, which could disrupt the stability of the Luttinger liquid phase. Of particular importance here is the possible generation of 'vortex operators' [13, 14, 15] which violate the conservation of the total number of $t$ or $p$ bosons obeyed by the terms so far included in $\mathcal{H}_{t,p}$. A simple analysis of the processes at higher orders in $w/V$ in terms of the $b$ bosons shows that such processes do indeed appear: the domain walls in the period-2 density-wave state, the $t$ bosons, can be annihilated or created in pairs. Similarly for the period-3 state, there are processes in which 3 $p$ bosons can be annihilated or created. We will examine the consequences of such processes by a combination of bosonization and Bethe ansatz methods. We will find that the vortex perturbations are indeed irrelevant at the $\sigma = -13/9$ critical point, so that there is a direct $z = 2$ transition from the gapped period-3 density-wave state, to a stable, gapless incommensurate phase. However, the vortex perturbations are found to be relevant at the $\sigma = -1/3$ critical point, implying that the gapless incommensurate phase does not extend all the way up to the period-2 density-wave state (see Fig. 8).

Here we study the stability of the Luttinger liquid phase of $\mathcal{H}_{t,p}$ postulated above within the framework of a long-wavelength bosonization analysis. This will allow us to place general conditions on the Luttinger parameters required for stability. This analysis will allow us to determine the values of the Luttinger parameters in some important limiting cases, and show there indeed exists an incommensurate phase stable to perturbation. The analysis does not allow us to determine the Luttinger parameter in general — this we will do in the following section by a Bethe ansatz analysis.

First, let us carry out the analysis using $\mathcal{H}_t$, and let us assume the value of $\sigma$ is such that we are in a compressible Luttinger liquid region. We follow the notation of Ref. 16, and introduce the continuum field $\theta_t$ with the action

$$\mathcal{S}_t = \frac{K_t}{2\pi v} \int dx d\tau \left[ (\partial_\tau \theta_t)^2 + v^2 (\partial_x \theta_t)^2 \right] \qquad (26)$$

Here $v$ is a velocity and $K_t$ is a Luttinger parameter, normalized so that free fermions have free fermions have $K = 1$. In terms of this field

$$t \sim e^{-i\theta_t}. \qquad (27)$$

Now the vortex operator $V \sim t^2 \sim e^{-2i\theta_t}$ is seen to have scaling dimension $1/K_t$ under the action $\mathcal{S}_t$, and hence the vortices are irrelevant, and the compressible phase is stable, as long as

$$K_t < \frac{1}{2}. \qquad (28)$$

We will determine the value of $K_t$ as a function of $\sigma$ in the following subsection, but here we note a simple where $K_t$ can be determined exactly. This is the limit where the density of $t$ bosons becomes vanishingly small as we approach the period-2 density-wave state with $\sigma \nearrow -1/3$. In this low density limit near a $z = 2$ quantum transitions, it can be shown that the $t$ particles behave like free fermions [12], and so we must have $K_t = 1$. The same argument can also be used to determine $v$ and so we have the important result

$$v = (w^2/V)\sqrt{-1 - 3\sigma} \quad ; \quad K_t = 1 \quad \text{as } \sigma \nearrow -1/3. \qquad (29)$$

Notice that $K_t$ does not obey (28), and hence vortices are always relevant at the boundary of the period-2 state, as we claimed above. As these vortices correspond to creation of pairs of the free fermions, the resulting fermion model is easily seen to be equivalent to the fermionized Ising model. This implies that we have an Ising transition at $\sigma = -1/3$ directly from the gapped period 2 ordered state to a disordered gapped state that does not break any symmetries, as shown in Fig 8.

Next, a complementary bosonization analysis can be applied to $\mathcal{H}_p$. We express the low energy physics using a Luttinger field $\theta_p$ with the action

$$\mathcal{S}_p = \frac{K_p}{2\pi v} \int dx d\tau \left[ (\partial_\tau \theta_p)^2 + v^2 (\partial_x \theta_p)^2 \right] \qquad (30)$$

As $\mathcal{H}_t$ and $\mathcal{H}_p$ have the same spectrum, the velocity $v$ should be the same as that in (26). However, the Luttinger parameter $K_p$ is now different because the interpretation of the field $\theta_p$ differs from (27):

$$p \sim e^{-i\theta_p} \qquad (31)$$

Now the vortex operator $V^\dagger \sim p^3$ has scaling dimension $9/(4K_p)$, and hence the vortices are irrelevant, and the compressible phase is stable, as long as

$$K_p < \frac{9}{8} \qquad (32)$$

Again, determination of the values of $K_p$ and $v$ requires a Bethe ansatz analysis, but exact results can be obtained in the limit $\sigma \searrow -13/9$, where the density of $p$ bosons becomes vanishingly small. The same arguments as applied above for the $t$ bosons now show that

$$v = (w^2/V)\sqrt{2(13 + 9\sigma)/9} \quad ; \quad K_p = 1 \quad \text{as } \sigma \searrow -13/9. \qquad (33)$$

Now $K_p$ does obey the stability condition (32), and hence vortices are always irrelevant at the boundary of the transition to the period-3 density-wave state. So, as claimed earlier, we have established the existence of a gapless, incommensurate state in this region. At some intermediate value of $\sigma$, the vortices will become relevant and will drive a Kosterlitz-Thouless transition to a gapped, disordered phase.

We conclude this subsection by noting that the relationship (23) implies a simple, general relationship between the Luttinger actions in (26) and (30). Indeed, the standard connection between particle density and the $\theta$ field in bosonization theory [16], combined with (23), leads to the condition

$$\frac{\theta_p}{\theta_t} = -\frac{2}{3}. \tag{34}$$

This result is also consistent with our expressions for the vortex operator $V$ noted below (27) and (31). Using (34) in (26) and (30), we also obtain the exact relationship

$$\frac{K_t}{K_p} = \frac{4}{9}, \tag{35}$$

which shows, not surprisingly, that the conditions (28) and (32) are the same.

## V. THE SIZE OF THE INCOMMENSURATE PHASE

To establish the boundaries of the incommensurate phase, we will show that the effective Hamiltonian (22) (or equivalently, (23)) can be solved using the Bethe ansatz. We will then use this to determine the Luttinger parameter anywhere in the incommensurate phase. The computation is a generalization of that done in [20] to cases with a "hard-core" constraint. Bethe ansatz analyses have been done in several related cases, the XXZ model with a hard core (not allowing down spins to be adjacent)[18], or a model of hard-core fermions arising in a supersymmetric chain [19]. The details of the computation of the Luttinger parameter have not been presented, however, so we describe the calculation in generality here.

### A. The Bethe ansatz

The $t$ boson in the effective Hamiltonian (22) is a kink which separates the two density-wave states. We denote the Ising-ordered state with no kinks as $|0\rangle$, so that an eigenstate of the Hamiltonian (37) with $N_t \leq N/3$ kinks is

$$\phi^{(N_t)} = \sum_{\{i_j\}} \varphi(i_1, i_2, \dots i_f) t^\dagger_{i_1} t^\dagger_{i_2} \dots t^\dagger_{i_f} |0\rangle \tag{36}$$

The $i_j$ are ordered so that $1 \leq i_1 < i_2 < \dots$, and moreover we require that $i_{j+1} - i_j = 3, 5, 7, \dots$; the Hamiltonian preserves this restriction. To simplify the analysis in this section, we shift away the constant term in $\mathcal{H}_t$, multiply by a constant, and define the effective chemical potential $h_t = -3(1+\sigma)/2$. This yields

$$H = -\sum_\ell \left[ \frac{1}{2}\left( t^\dagger_{\ell+2} t_\ell + t^\dagger_\ell t_{\ell+2} \right) + h_t t^\dagger_\ell t_\ell + \frac{1}{3} t^\dagger_{\ell+3} t_{\ell+3} t^\dagger_\ell t_\ell \right]. \tag{37}$$

This Hamiltonian has the same eigenvectors as the original. For simplicity, we also assume periodic boundary conditions.

Bethe's ansatz is that the state $\phi^{(N_t)}$ is of the form

$$\varphi(i_1, i_2, \dots i_{N_t}) = \sum_P A_P \, \mu^{i_1}_{P1} \mu^{i_2}_{P2} \dots \mu^{i_{N_t}}_{PN_t}. \tag{38}$$

for some numbers $\mu_j$ and $A_P$, where $j = 1, \dots, N_t$ and $P \equiv (P1, P2, \dots, PN_t)$ is a permutation of the integers $(1, 2, \dots, N_t)$. With periodic boundary conditions, we can construct eigenstates of the translation operator $T$, which sends $T t^\dagger_{i_1} t^\dagger_{i_2} \dots = t^\dagger_{i_1+1} t^\dagger_{i_2+1} \dots$. A state obeying Bethe's ansatz is an eigenstate of $T$ if the amplitudes $A_P$ are cyclically related as

$$A_{PN_t, P1, P2, \dots P(N_t-1)} = \mu^N_{PN_t} A_{P1, P2, \dots PN_t}. \tag{39}$$

If we define the bare momenta $k_j$ via $\mu_j \equiv e^{-ik_j}$, the eigenvalue $e^{ik_{\rm tot}}$ of $T$ is then given by

$$k_{\rm tot} = -i \ln \left[ \prod_{j=1}^{N_t} (\mu_j)^{-1} \right] = \sum_{j=1}^{N_t} k_j \tag{40}$$

The relation (39) then can be thought of as the quantization of the momentum of a particle in a box.

The $\mu_i$ and the amplitudes $A_P$ are found by demanding that $\phi^{(N_t)}$ be an eigenstate. It is simplest to illustrate this in the case of two kinks. The Bethe ansatz is that

$$\begin{aligned} \varphi(i_1, i_2) &= \sum_P A_P \, \mu^{i_1}_{P1} \mu^{i_2}_{P2} \\ &= A_{12} \mu^{i_1}_1 \mu^{i_2}_2 + A_{21} \mu^{i_1}_2 \mu^{i_2}_1 \end{aligned}$$

Requiring $\phi^{(2)}$ be an eigenstate of $T$ means that

$$A_{12} = A_{21} \mu^N_1,$$

with $e^{-ik_{\rm tot}} = \mu_1 \mu_2$. Operating with the Hamiltonian (37) on $\phi^{(2)}$ yields

$$H\phi^{(2)} = E_t \phi^{(2)} + \sum_{i=1}^{N} X_i t^\dagger_i t^\dagger_{i+3}$$

where

$$E_t = -h_t N_t - \frac{1}{2}\left[ \mu^2_1 + \mu^2_2 + (\mu_1)^{-2} + (\mu_2)^{-2} \right].$$

and

$$X_i = -\frac{2}{3}\varphi(i, i+3) + \varphi(i, i+1) + \varphi(i+2, i+3).$$

The Bethe equations are derived by requiring that all the $X_i$ vanish, so that $\phi^{(2)}$ is an eigenstate. With the Bethe ansatz, this means that

$$X_i = -\sum_P A_P\, \mu_{P1}^i \mu_{P2}^i \left(2\Delta \mu_{P2}^3 - \mu_{P2} - \mu_{P1}^2 \mu_{P2}^3\right) = 0$$

where $\Delta = 1/3$. Each of these vanishes if

$$\frac{A_{21}}{A_{12}} = -\frac{\mu_2}{\mu_1}\frac{\mu_2^2\mu_1^2 + 1 - 2\Delta\mu_2^2}{\mu_2^2\mu_1^2 + 1 - 2\Delta\mu_1^2}.$$

Combining this with the periodic boundary conditions (39) yields

$$\frac{A_{12}}{A_{21}} = \mu_1^N = -\frac{\mu_1(\mu_1^2\mu_2^2 + 1 - \mu_1^2)}{\mu_2(\mu_1^2\mu_2^2 + 1 - \mu_2^2)}.$$

Let $\nu_j = \mu_j^2$. Then using the fact that $e^{-ik_{\rm tot}} = \mu_1\mu_2$ gives the Bethe equation

$$\nu_m^{(N-2)/2} e^{-ik_{\rm tot}} = -\frac{\nu_m\nu_j + 1 - \nu_m}{\nu_m\nu_j + 1 - \nu_j},$$

which holds for $(m,j) = (1,2)$ and $(2,1)$. One solves these two equations for $\nu_1$ and $\nu_2$ subject to the constraint $e^{-2ik_{\rm tot}} = \nu_1\nu_2$. Then the corresponding eigenstate is found (up to an overall constant) by substituting the values of $\nu_i$ into the equation for $A_{21}/A_{12}$.

This computation can be generalized to any number of kinks $N_t$. The constraint that $\phi^{(N_t)}$ be an eigenstate is basically the same as the two-kink case: one requires that

$$\begin{aligned} 0 \;=\; & 2\Delta\varphi(...,i,i+2,...) - \varphi(...,i,i+1,...) \\ & -\varphi(...,i+1,i+2,...) \end{aligned}$$

for any choice of $i_1, i_2, \ldots i_{N_t}$ and $i$. The trick to make this vanish is to consider the permutation $P'$, which differs from $P$ only in that $Pm$ and $P(m+1)$ are reversed, i.e. $P' = P1P2\ldots P(m-1)P(m+1)PmP(m+2)\ldots PN_t$. Therefore $\phi^{(N_t)}$ is an eigenstate if for all $P$ and $m$

$$\frac{A_{P'}}{A_P} = g(\nu_{P(m+1)}, \nu_{Pm}) \tag{41}$$

with

$$g(a,b) \equiv -\frac{\sqrt{a}(ab + 1 - 2\Delta a)}{\sqrt{b}(ab + 1 - 2\Delta b)}.$$

One can think of $g$ as the bare S-matrix describing the phase shift when two kinks are interchanged. The fact that $g(a,a) = -1$ means that the wavefunction vanishes if two of the bare momenta $k_j$ are identical. To find the $\nu_j$, we impose the boundary condition (39). Note that

$$\begin{aligned} \frac{A_{PN_t,P1\ldots P(N_t-1)}}{A_{P1,P2,\ldots PN_t}} \;&=\; \frac{A_{P1,PN_t,P2\ldots P(N_t-1)}}{A_{P1,P2\ldots PN_t}} g(\nu_{PN_t},\nu_{P1}) \\ &=\; \prod_{j=1}^{N_t} g(\nu_{PN_t},\nu_{Pj}) \end{aligned}$$

The condition (39) must hold for all $PN_t$, and hence all $j$. Putting this all together yields the Bethe equations for the $\mu_j$ or $\nu_j$:

$$\nu_j^{N/2} = \prod_{m=1}^{N_t} g(\nu_j,\nu_m).$$

This is thus a coupled set of polynomial equations for the $\mu_i$. Using the explicit form of $g$, and the expression (40) for the translation eigenvalue $e^{ip}$, the Bethe equations simplify to

$$\nu_j^{(N-N_t)/2} e^{-ik_{\rm tot}} = (-1)^{N_t-1} \prod_{m=1}^{N_t} \frac{\nu_j\nu_m + 1 - 2\Delta\nu_j}{\nu_j\nu_m + 1 - 2\Delta\nu_m}. \tag{42}$$

These are a set of $N_t$ coupled polynomial equations for the $\nu_j = e^{2ik_j}$, $j = 1\ldots N_t$. Solving these for a set of $k_j$, one then finds the corresponding eigenstate (up to an overall normalization) by using (41). This eigenstate has energy

$$E_t = -h_t N_t - \sum_{j=1}^{N_t} \cos(2k_j) \tag{43}$$

These are precisely the Bethe equations and energy one obtains for the XXZ model at $\Delta = J_z/J_x = 1/3$ with $(N - N_t)/2$ sites, if one imposes twisted boundary conditions resulting in the factor of $e^{-ik_{\rm tot}}$ in (42). The twist and the different number of sites result from the excluded-volume effect (the restriction that $t$ bosons must be $3, 5, 7, \ldots$ sites apart), and the fact that $t$ bosons hop two sites instead of one.

In the next subsection we will use these Bethe equations to find the size of the incommensurate phase. Since we saw by using bosonization that the incommensurate region is closer to the $\mathbf{Z_3}$-ordered phase than to the $\mathbf{Z_2}$-ordered phase, the density of $p$ bosons in the incommensurate phase will be much smaller than that of the $t$ bosons. It is thus useful to derive the Bethe equations in the $p$ boson basis. The analogous wavefunction $\widetilde{\varphi}$ must obey

$$\begin{aligned} 0 \;=\; & 2\Delta\widetilde{\varphi}(...,i,i+2,...) - \widetilde{\varphi}(...,i,i-1,...) \\ & -\widetilde{\varphi}(...,i+3,i+2,...) \end{aligned}$$

with, crucially, the same $\Delta = 1/3$ as for the $t$ bosons. Going through a virtually-identical calculation yields

$$e^{3ik_{\rm tot}} = \prod_{j=1}^{N_p} \omega_j$$

$$E_p = -h_p N_p - \frac{1}{2}\sum_{j=1}^{N_p} \left[\omega_j + \omega_j^{-1}\right] \tag{44}$$

$$\omega_j^{(N+N_p)/3} e^{ik_{\rm tot}} = (-1)^{N_p-1} \prod_{m=1}^{N_p} \frac{\omega_j\omega_m + 1 - 2\Delta\omega_j}{\omega_j\omega_m + 1 - 2\Delta\omega_m}. \tag{45}$$

where the effective chemical potential here is $h_p = \sigma + 4/9$. Note that the right-hand-side of the Bethe equations here are identical to those for the $t$ bosons (and for the corresponding XXZ model); only the left-hand-side changes.

### B. Calculation of the Luttinger parameter

Since a great deal of discussion of the size of the incommensurate phase has appeared in the literature (see e.g. [13, 14, 15]), we feel it is worth discussing in detail a case where the answer can be determined exactly via the Bethe ansatz. In this subsection we therefore derive explicitly the size of the incommensurate phase by finding the range of $\sigma$ where the vortex operators are irrelevant. We do this by computing the Luttinger parameters $K_p = 9K_t/4$ of the effective Hamiltonian. The dimension of operators can be computed directly by using either the asymptotics of the correlator [21] or finite-size effects [22], but the result is identical. In this subsection, we will generalize Haldane's computation of the Luttinger parameter [20] to the case at hand. The computation we do here is more complicated because the exponent on the left-hand-side of (42) or (45) depends on the number of kinks in the system. This is a consequence of the restrictions on the locations of the particles: more particles effectively reduces the size of the system.

The XXZ spin chain at $\Delta = 1/3$ is in a gapless phase. The vortex operators are forbidden from occuring because of the $U(1)$ symmetry of the spin chain; if one breaks this symmetry by allowing e.g. $J_x \neq J_y$, then the resulting XYZ chain is indeed gapped. One can show using the above Bethe ansatz computation that Hamiltonians (22) and (23) are also in a gapless phase: the slight difference in Bethe equations does not change this result. This difference, however, does complicate the computation of the dimension of the vortex operators. It also means that as opposed to the XYZ model, there is a gapless phase with broken $U(1)$ symmetry and irrelevant vortex operators. In a gapless phase, the Luttinger parameter $K_p$ is defined by the general relation [16]

$$\frac{\pi v}{K_p} = \frac{\partial^2 E_p}{\partial N_p^2} \tag{46}$$

where $E_p$ is given in (44), and $v$ is the velocity of the excitations. Using the fact that $3N_t + 2N_p = N$ means that $K_p = 9K_t/4$, as noted above.

To do this computation, it is convenient to rewrite the Bethe equations in terms of "rapidity" variables $\theta_j$. These are defined by the relation

$$\omega_j \equiv e^{-3ik(\theta_j)} \equiv -\frac{\sinh(\theta_j + i\gamma/2)}{\sinh(\theta_j - i\gamma/2)}$$

where $\gamma = \cos^{-1}(-\Delta)$; for our models, $\Delta = 1/3$. This relation also defines $k$ as a function of $\theta$, i.e. $k_j \equiv k(\theta_j)$. This change of variables from momentum to rapidity is useful because it puts the Bethe equations (45) in difference form: taking the log of both sides gives

$$(2M_j + 1)\pi = RNk(\theta_j) - \lambda k_{\rm tot} + \sum_{m=1}^{N_p} L(\theta_j - \theta_m) \tag{47}$$

where $M_j$ is an integer, and

$$L(\theta) = i \ln\left[\frac{\sinh(\theta + i\gamma)}{\sinh(\theta - i\gamma)}\right].$$

We have defined the parameters $R$ and $\lambda$ to make the analysis apply to general models with hard-core constraints. For the $p$ bosons we have $R = 1 + N_p/N$ and $\lambda = 1$. For the $t$ bosons, we have $R = 1 - N_t/N$ and $\lambda = -1$. The usual XXZ model has $R = 1$ and $\lambda = 0$. The cases discussed in [18, 19] can also be written in this form.

Each kink is characterized by an different integer $M_j$; if one were to have $M_j = M_m$ for $j \neq m$, then $\theta_j = \theta_m$, and we showed above that identical bare momenta results in the Bethe ansatz wavefunction vanishing. Summing (47) over $j$ and using the fact that $L(\theta) = -L(-\theta)$ means that the total momentum is

$$k_{\rm tot} = \frac{1}{N}\sum_j (2M_j + 1)\pi. \tag{48}$$

The $\theta_j$ in the ground state are all real, and lie in the region $|\theta_j| \leq \Lambda$, where $\Lambda$ depends on the chemical potential $h$. There is one particle in the ground state for each solution of (47) with $|\theta_j| \leq \Lambda$; removing any particle in this region increases the energy.

To make any more progress, one needs to go to the thermodynamic limit, where there are many particles, and the rapidities are closely spaced together. We then define the density of particles $\rho(\theta)$ so that $N\rho(\theta)d\theta$ gives the number of particles in the ground state with rapidities between $\theta$ and $\theta + d\theta$. In the ground state, there is a particle associated with each integer $M_j$, as long as the rapidity is below $\Lambda$. For $|\theta| < \Lambda$, the equations (47) therefore become

$$2\pi\rho(\theta) = Rk'(\theta) + \int_{-\Lambda}^{\Lambda} d\theta'\ \Phi(\theta - \theta')\rho(\theta') \tag{49}$$

where $\Phi(\theta) \equiv L'(\theta)$. The integral equation (49) determines the ground-state density $\rho(\theta)$ for a particular $\Lambda$. The maximum rapidity $\Lambda$ depends on $h_p$, and is determined by minimizing the energy (44), subject to $\rho(\theta)$ obeying (49). In the thermodynamic limit, the ground-state energy is

$$E_p = N\int_{-\Lambda}^{\Lambda} d\theta\ \rho(\theta)\epsilon_0(\theta) \tag{50}$$

where the bare energy of a kink is

$$\epsilon_0(\theta) = -h_p - \Delta - \frac{\sin^2(\gamma)}{\cosh(2\theta) - \cos(\gamma)}.$$

The minimum value of the last term in $\epsilon_0$ is $-(1+\cos\gamma) = \Delta - 1$, so if $h_p \leq -1$, it becomes energetically favorable to have an empty ground state. Converting back to the original variables, this is the Pokrovsky-Talapov transition occuring at $\sigma = -13/9$.

Even though the density $\rho(\theta)$ and the largest rapidity $\Lambda$ completely characterize the system at zero temperature, extracting the Luttinger parameter requires further work. We first compute the velocity $v$ of the excitations. We define $E_{\rm hole}(\theta_h)$ and $k_{\rm hole}(\theta_h)$ as the energy and momentum change in the system resulting from removing a particle of rapidity $\theta_h$ from the ground state. The velocity is then

$$v = \left.\frac{\partial E_{\rm hole}}{\partial k_{\rm hole}}\right|_{\theta_h=\Lambda} = \left.\frac{\partial E_{\rm hole}/\partial\theta_h}{\partial k_{\rm hole}/\partial\theta_h}\right|_{\theta_h=\Lambda}$$

Say we remove the particle associated with integer $M_h$ and rapidity $\theta_h$. Because the particles are coupled, the momenta of all of them changes when a particle is removed. However, the integers $M_j$ do not change, so from (48), we see that $k_{\rm hole} = -(2M_h+1)\pi/N$. Using (47), we can rewrite this in the thermodynamic limit in terms of the rapidities. After a few manipulations, we have

$$\frac{\partial k_{\rm hole}}{\partial\theta_h} = -2\pi\rho(\theta_h) \tag{51}$$

just as in the case without hard cores.

The energy of a hole of rapidity $\theta_h$ is

$$E_{\rm hole}(\theta_h) = -\epsilon_0(\theta_h) + \sum_{j\neq h}\epsilon_0'(\theta_j)\delta\theta_j.$$

where $\delta\theta_j$ is the change in rapidity of particle $j$ when the hole is created. Because the integers $M_j$ do not change, (47) requires that

$$\begin{aligned} 0 \;=\; & RNk'(\theta_j)\delta\theta_j + \lambda k(\theta_j) - \lambda k_{\rm hole} - L(\theta_j-\theta_h) \\ & + \sum_{m\neq h}\Phi(\theta_j-\theta_m)(\delta\theta_j - \delta\theta_m). \end{aligned}$$

Taking the thermodynamic limit and using (49) simplifies this to an integral equation:

$$\begin{aligned} 2\pi N\rho(\theta)\delta\theta(\theta;\theta_h) \;=\; & L(\theta-\theta_h) - \lambda k(\theta) + \lambda k_{\rm hole}(\theta_h) \\ & -N\int_{-\Lambda}^{\Lambda} d\theta'\,\Phi(\theta-\theta')\rho(\theta')\delta\theta(\theta';\theta_h). \end{aligned}$$

Note that $\delta\theta$ is a function of both $\theta$ and $\theta_h$. Let us define the function $\tau(\theta)$ as the solution of the integral equation

$$2\pi\tau(\theta) = -\Phi(\theta-\Lambda) + \int_{-\Lambda}^{\Lambda} d\theta'\,\Phi(\theta-\theta')\tau(\theta'). \tag{52}$$

We then have

$$\begin{aligned} & N\frac{\partial}{\partial\theta_h}\left[\rho(\theta)\delta\theta(\theta;\theta_h) - \rho(-\theta)\delta\theta(-\theta;\theta_h)\right]\Big|_{\theta_h=\Lambda} \\ & \qquad = \tau(\theta) - \tau(-\theta) \end{aligned}$$

because $k_{\rm hole}(\theta_h)$ is odd in $\theta_h$. Because $\epsilon_0'(\theta)$ is odd in $\theta$, we use this with expression for hole energy to get

$$\left.\frac{\partial E_{\rm hole}}{\partial\theta_h}\right|_{\theta_h=\Lambda} = -\epsilon_0'(\Lambda) + \int_{-\Lambda}^{\Lambda} d\theta\;\epsilon_0'(\theta)\tau(\theta) \tag{53}$$

As with $k_{\rm hole}$, this is the same as in the case without hard cores. Combining this with (51) gives the velocity of the excitations. We can check this by noting that as $\sigma \to -13/9$, there are no $p$ bosons in the ground state. This means that $\Lambda \to 0$, so it follows from (53), (51) and (49) that $v \to \epsilon_0'(0)/k'(0) = 0$. The quasiparticles here have dispersion $E_{\rm hole} \propto k_{\rm hole}^2$, as expected at a $z = 2$ Pokrovsky-Talapov transition.

The computation of the Luttinger parameter (46) is affected by the hard-exclusion effects. In particular, because $R = (1+N_p/N)/3$ in (49) depends on the number of particles $N_p$, $\partial R/\partial\Lambda \neq 0$. First we compute how the number of particles changes when $\Lambda$ is varied. It is convenient to define the rescaled density $\widetilde{\rho} = \rho/R$, so that for fixed $\Lambda$, $\widetilde{\rho}$ is independent of $R$. Then if we define $\chi(\theta)$ as the solution of the integral equation

$$2\pi\chi(\theta) = L(\theta-\Lambda)+L(\theta+\Lambda)+\int_{-\Lambda}^{\Lambda} d\theta'\Phi(\theta-\theta')\chi(\theta') \tag{54}$$

it is straightforward to show that

$$\frac{\partial\widetilde{\rho}(\theta)}{\partial\Lambda} = \frac{\widetilde{\rho}(\Lambda)}{1-\chi(\Lambda)}\frac{\partial\chi(\theta)}{\partial\theta}.$$

Because

$$N\int_{-\Lambda}^{\Lambda} d\theta\,\widetilde{\rho}(\theta) = \frac{N_p}{R} = \frac{N_p}{1+N_p/N},$$

we have

$$N_p' \equiv \frac{\partial N_p}{\partial\Lambda} = NR^2\frac{2\widetilde{\rho}(\Lambda)}{1-\chi(\Lambda)}.$$

To compute the Luttinger parameter, it is convenient to also define a rescaled energy $\widetilde{E} = E_p/R$. A little algebra then yields

$$\frac{\partial^2 E_p}{\partial N_p^2} = \frac{1}{RN_p'}\frac{\partial}{\partial\Lambda}\left(\frac{\widetilde{E}'R^2}{N_p'}\right)$$

where $\widetilde{E}' \equiv \partial\widetilde{E}/\partial\Lambda$. Computing $\widetilde{E}'$ is then similar to the $R = 1$ case of [20], yielding

$$\frac{\partial^2 E_p}{\partial N_p^2} = \frac{1}{RN_p'}\frac{\partial}{\partial\Lambda}\left(\epsilon_0(\theta) - \frac{1}{2}\int_{-\Lambda}^{\Lambda}\epsilon_0'(\theta)\chi(\theta)\right).$$

Since none of the quantities inside the derivative depends on $R$, we can use the calculation of [20] to get

$$\frac{\partial^2 E_p}{\partial N_p^2} = \frac{1}{R^3}\frac{(1-\chi(\Lambda))^2}{2\widetilde{\rho}(\Lambda)}\left(\epsilon_0'(\theta) - \int_{-\Lambda}^{\Lambda}\epsilon_0'(\theta)\tau(\theta)\right)$$

where $\tau(\theta)$ is defined above via (52). Combining this with our computation of the velocity above yields finally the Luttinger parameter

$$K_p = \left( \frac{1 + N_p/N}{1 - \chi(\Lambda)} \right)^2 \tag{55}$$

The effect of the hard-core constraints ends up being the $(1 + N_p/N)^2$ in the numerator.

We have seen that when the coupling $\sigma = -13/9$, there are no $p$ bosons in the ground state. The equation (55) gives the correct $K_p = 1$, because $\chi(0) = 0$ and $N_p = 0$ here. As $\sigma$ is increased, $p$ bosons with $|\theta| \leq \Lambda$ fill the ground state. For some value of $\sigma$, $\Lambda \to \infty$. We can find out how many bosons there are here, because in this limit we can solve the equation (49) by Fourier transformation. Actually, to just get $N_p(\Lambda \to \infty)$, we do not need to go to the trouble: we know from the XXZ model that

$$\lim_{\Lambda \to \infty} \int_{-\Lambda}^{\Lambda} d\theta \, \widetilde{\rho}(\theta) = \frac{1}{2}.$$

Thus in our case, we have $N_p(\Lambda \to \infty) = N/5$. The equation (55) for the Luttinger parameter is therefore valid only for values of chemical potential such that only solutions of the Bethe equations with all bare momenta real are present in the ground state. In other words, (55) is valid only for $\sigma$ such that $N_p \leq N/5$. To find the Luttinger parameter for the remaining range of $\sigma$, we can repeat the above analysis for the $t$ bosons. This yields

$$K_t = \left( \frac{1 - N_t/N}{1 - \chi(\Lambda_t)} \right)^2, \tag{56}$$

where $\Lambda_t$ is the maximum rapidity of a $t$ boson in the ground state. By the same argument, this expression is valid for $N_t \leq N/5$.

Because $2N_p + 3N_t = N$, the expressions for the Luttinger parameter are both valid at exactly one point: where $\Lambda = \Lambda_t = \infty$, $N_p = N_t = 1/5$. This provides a good check on our result: at $\Lambda = \Lambda_t = \infty$, $N_p = N_t = 1/5$, comparing the expressions (55) and (56) yields $K_t = 4K_p/9$, as noted in general in (35). In fact, we can find the exact value of $K_p$ at this point, by either a Weiner-Hopf analysis [21], or by appealing to the XXZ model, where the answer is known. Either way, one finds that

$$\lim_{\Lambda \to \infty} (1 - \chi(\Lambda))^2 = 2 \cos^{-1}(\Delta)/\pi$$

For our case of $\Delta = 1/3$, we have therefore $K_p = 1.83754$, so vortices are relevant here. Another check on our results is to note that the computation of the velocity $v$ must give the same answer at this point whether computing with the $t$ bosons or the $p$ bosons. Indeed, we see from (51) and (53) that both are independent of $R$ and $\lambda$, only depending on $\Lambda$; since $\Lambda$ is the same for both pictures, we do get the same answer.

The incommensurate regime is characterized by having $K_p < 9/8$. We cannot analytically find the value of $\sigma$ where $K_p = 9/8$, but it is straightforward to solve the above integral equations numerically. First, one must determine the value of $\Lambda$ for a given $\sigma$ by solving (49) for $\rho(\theta)$ and $\Lambda$ while demanding that the energy (50) be minimized. Integrating $\rho(\theta)$ yields the ground-state particle density $N_p/N$ as well. Knowing $\Lambda$ then allows one to solve (54) for $\chi(\theta)$ and hence $\chi(\Lambda)$. Plugging this into (55) then yields the Luttinger parameter. We find that $K_p = 9/8$ when $\sigma = 1.422....$ This leads to our final result for the phase diagram: the incommensurate phase exists only for

$$1.422 < \sigma < 1.444 \ .$$

The incommensurate region is also very narrow near the Potts critical point $M_3$, so it is likely that it occupies a very small region of parameter space. We plot $K_p$ as obtained above in Fig 9.

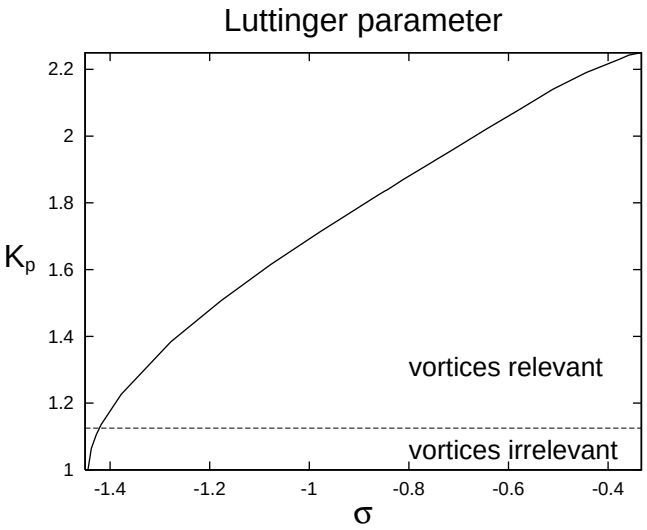


FIG. 9: Bethe ansatz results for $K_p$ as a function of $\sigma$. Recall that $K_t = 4K_p/9$.

## VI. CONCLUSION

The primary purpose of this paper was to provide a thorough study of the very simple one-dimensional boson model in (3). This model was originally motivated by the studies of 'tilted' Mott insulators of atoms in optical lattices. Despite its simplicity, our model has a rich phase diagram, shown in Fig 1, with a many competing ordered phases and possibilities for exact solutions.

Our solutions shed additional light on the nature of the phase transition in the chiral clock model. Over a certain regime of parameters, we provide definitive evidence for a gapless, floating incommensurate phase adjacent to the gapped $\mathbf{Z}_3$ ordered phase with a period-3 density wave. However, the size of this incommensurate phase was remarkably small, making it unlikely that it will ever be

observed in experimental or numerical studies. We also obtained specific realizations of two of the exactly soluble multi-critical points identified by Andrews *et al.* [23], which are now known to be part of the series of minimal conformal models [6]. It is likely that our analysis could be generalized to this series; it would be interesting in particular to see if the incommensurate phases existed in general.

### Acknowledgments

We are very grateful to David Huse and Nick Read for a number of useful comments. This research was supported by US NSF grants DMR-0098226 (K.S. and S.S.) DMR-0104799 (P.F.), and by a DOE grant DEFG02-97ER41027 (P.F.). P.F. and S.S. would also like to thank the Aspen Center for Physics for hospitality during part of this work.

## APPENDIX: CONNECTION TO BAXTER'S HARD SQUARE MODEL

In this appendix we show that the quantum Hamiltonian $\mathcal{H}$ in (3) generates precisely the transfer matrix of the classical, two-dimensional hard-square model introduced by Baxter [3].

It is useful to note that the hard-square model, as defined in the Introduction, can also be interpreted as a certain 'interface' or 'height' model. In particular, it is identical to the so-called $A_4$ restricted-solid-on-solid (RSOS) [23]. To see the connection with the RSOS model, we need to associate each tile configuration with a corresponding set of heights. On one sublattice of the square lattice, associate each site with a tile present with height 1, and a vacancy with height 3. On the other sublattice, associate each tile with height 4, and a vacancy with height 2. Then the hard-square restrictions are simply encoded in a set of constraints on heights on nearest neighbor sites: height 1 can only be next to 2, 2 can be next to 3 or 1, 3 can only be next to 2 or 4, and 4 can only be next to 3. These height restrictions are conveniently summarized in the $A_4$ Dynkin diagram, and hence the terminology. Like the hard-square case, the general $A_n$ RSOS models are solvable along two lines, with one critical point on each. These critical points are multicritical points with known conformal-field-theory descriptions [6].

Here, we continue to use the terminology of hard squares. We consider the diagonal-to-diagonal transfer matrix of the hard square model. In the orientation of Fig. 11, this transfer matrix acts on the space of states of a zig-zag line of lattice sites as shown in Fig. 10.

There are three interaction parameters: $L$ and $M$ are the interaction strength of adjacent tiles, while $z$ is the fugacity for each tile. The grand canonical partition function can then be written as the sum of products of

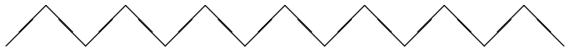

FIG. 10: Zig-zag line defining the space of states upon which $\mathcal{H}$ acts.

Boltzmann weights. The Boltzmann weight of a plaquette is shown in Fig. 11 where the heights $a, b, c$ and $d$

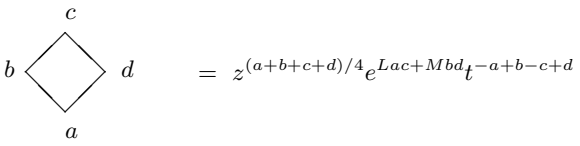


FIG. 11: Boltzmann weight of a plaquette of the square lattice. The tiles are centered on the vertices of this plaquette, and $a, b, c, d = 0, 1$ indicates absence/presence of a tile.

are 0 or 1; 1 denotes a tile, so the restriction is that $ab = bc = cd = da = 0$. The extra parameter $t$ cancels out of the partition function and so is arbitrary. The pure hard square model is obtained by setting $L = M = 0$, but we will need the full range of values of these couplings to explore the parameter space of $\mathcal{H}$. The hard-hexagon model (on a triangular lattice) is obtained by setting $L = 0$ and $M \to -\infty$.

We will now take the so-called $\tau$-continuum limit of this transfer matrix, so that we may obtain the corresponding Hamiltonian which evolves the states in a continuous imaginary time. To take this Hamiltonian limit, we define $t = \exp(L/4)$ and $z = e^{-L}(1 - \zeta)$. Then the Boltzmann weights for all the allowed possible states around each plaquette are shown in Fig. 12.

When $\zeta = M = 0$ and $L \to \infty$, the vertical transfer matrix is the identity. The Hamiltonian is found by expanding around this limit. The small parameters are then $\zeta$, $M$ and $e^{-L/2}$. Note that to get back to the original Hilbert space, we need to break the transfer matrix into two pieces. The first evolves the lower of the two rows of sites in the above zig-pattern, and then the second evolves the upper row. The full transfer matrix is then

$$T_1 T_2 \approx (1 - \zeta\mathcal{H}_1)(1 - \zeta\mathcal{H}_2) \approx (1 - \zeta\mathcal{H}), \qquad \text{(A.1)}$$

where $\mathcal{H} = \mathcal{H}_1 + \mathcal{H}_2$. Let $d_j^\dagger$ be a boson creation operator which creates a tile on site $j$. We identify these tiles with the bosons of (3). It is easy to see that the constraints of the hard square model correspond precisely to the constraints (2). Moreover, here we obtain the same Hamiltonian in (3) (up to an arbitrary overall energy scale) with the couplings

$$\frac{U}{w} = e^{L/2}\zeta \quad ; \quad \frac{V}{w} = -Me^{L/2} \qquad \text{(A.2)}$$

Note that $M > 0$ means attractive next-nearest-neighbor interactions.

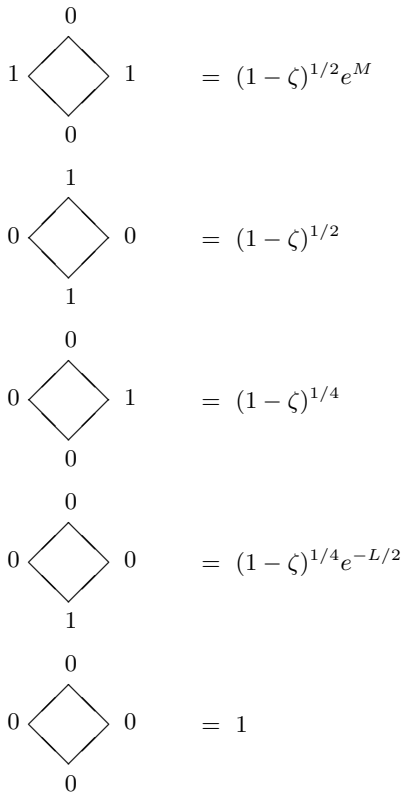


FIG. 12: Boltzmann weights for the possible states of a plaquette of the hard square model

Baxter [3] showed that the hard-square model is integrable for

$$z = \frac{(1-e^{-L})(1-e^{-M})}{e^{L+M}-e^{L}-e^{M}}. \tag{A.3}$$

In the Hamiltonian limit, this condition is equivalent to (4). Baxter also showed that there are two critical points within the parameter space of (A.3). Defining

$$I = z^{-1/2}(1-ze^{L+M}),$$

the critical points are at

$$I = \pm\left[\frac{1+\sqrt{5}}{2}\right]^{-5/2},$$

which leads to (6,8). The critical point at (6) is in the universality class of the tricritical Ising model, while that at (8) is of the 3-state Potts type [3, 4]. The physical interpretation of these critical points is discussed in Section II.


[1] S. Sachdev, K. Sengupta and S. M. Girvin, Phys. Rev. B, **66** 075128 (2002).
[2] M. Greiner, O. Mandel, T. Esslinger, T. W. Hänsch, and I. Bloch, Nature (London) **415**, 39 (2002).
[3] R. J. Baxter, J. Phys. A 13, L61 (1980); J. Stat. Phys **26**, 427 (1981); *Exactly Solved Models in Statistical Mechanics* (Academic, London, 1982).
[4] D. A. Huse, Phys. Rev. Lett. **49** 1121 (1982); J. Phys. A **16** 4369 (1983).
[5] R. J. Baxter and P. A. Pearce, J. Phys. A **15**, 897 (1982); J. Phys. A **16**, 2239 (1983).
[6] D. A. Huse, Phys. Rev. B **30**, 3908 (1984).
[7] P. Lecheminant and E. Orignac, cond-mat/0309345
[8] S. Ostlund, Phys. Rev. B **24**, 398 (1981).
[9] D. A. Huse and M. E. Fisher, Phys. Rev. Lett. **49**, 793 (1982).
[10] J. L. Cardy, Nucl. Phys. B **389**, 577 (1993).
[11] V.L. Pokrovsky and A.L. Talapov, Phys. Rev. Lett. **42**, 65 (1979).
[12] S. Sachdev, T. Senthil, and R. Shankar, Phys. Rev. B **50**, 258 (1994).
[13] F.D.M. Haldane, P. Bak, and T. Bohr, Phys. Rev. B **28**, 2743 (1983).
[14] H.J. Schulz, Phys. Rev. B **28**, 2746 (1983).
[15] J. Villain and P. Bak, J. Physique **42**, 657 (1981).
[16] *Quantum Phase Transitions*, by S. Sachdev, Cambridge University Press, Cambridge (1999), Chapter 14.
[17] F. Y. Wu, Rev. Mod. Phys. **54**, 235 (1982).
[18] F.C. Alcaraz and R.Z. Bariev, [cond-mat/9904042]; I.N. Karnaukhov and A.A. Ovchinnikov, Eur. Phys. Lett. **57** (2002) 540 [cond-mat/0110289].
[19] P. Fendley, B. Nienhuis and K. Schoutens, [cond-mat/0307338].
[20] F. D. M. Haldane, Phys. Lett. A **81**, 153 (1981).
[21] N. M. Bogoliubov, A. G. Izergin, and V. E. Korepin, Nucl. Phys. B **275**, 687 (1986).
[22] F. Woynarovich, H. P. Eckle, T.T. Truong, J. Phys. A **22**, 4027 (1989).
[23] G. E. Andrews, R. J. Baxter, and P. J. Forrester, J. Stat. Phys. **35**, 193 (1984).